

**EFFECT OF CRYSTALLOGRAPHIC TEXTURE ON CAVITATION WEAR RESISTANCE OF As-CAST CuZn10 ALLOY**

Analysis of a crystallographic texture (a preferred orientation) effect on cavitation wear resistance of the as-cast CuZn10 alloy, has been conducted in the present paper. The experiment was conducted on the CuZn10 alloy samples with  $\langle 101 \rangle // ND$  or  $\langle 111 \rangle // ND$  preferred orientations (where the ND denotes direction that is perpendicular to the exposed surface). The cavitation resistance examinations have been carried out on three different laboratory stands (namely, vibration, jet-impact and flow stands) that are characterized by a various intensity and a way of cavitation's excitement. Obtained results point towards a higher cavitation resistance of the CuZn10 alloy with the  $\langle 111 \rangle // ND$  preferred orientation.

*Keywords:* texture, cavitation, cavitation erosion, electron backscatter diffraction (EBSD), CuZn10 alloy

**1. Introduction**

The action of pressure pulses on a material's surface leads to a cavitation damage. Thus, the cavitation process is composed of a formation, a growth and an implosion of bubbles induced by cyclical pressure changes in a flowing liquid [1-3].

The bubbles containing an evaporated liquid or a mixture of gases are formed in low-pressure regions, and then implode in a vicinity of high-pressure zones leading to a the material's erosion. A kind of bubbles' filling, a way of excitement and an intensity of cavitation play a crucial role in determining a material's resistance to the cavitation phenomenon. In the case of flowing liquid devices, where cavitation bubbles are filled with non-dissolved gases, the destruction goes with "gentle" conditions. This "gentle" course is an effect of a diffusion of a large quantity of steam to the vicinity of cavitation bubbles in high pressure zones. On the other hand, an acoustic cavitation that exhibit an aggressive and dynamic course is considered as "hard" [4-6].

In this paper, the effect of crystallographic texture on cavitation resistance of the as-cast CuZn10 alloy tested on three various laboratory stands (namely, vibration, jet-impact and flow stands), is analyzed.

**2. Investigated materials**

The material investigated was a CuZn10 alloy. The alloy was fabricated by a melting of pure elements (Cu cathode

and 99,995% zinc) in PIT10 induction furnace. CuZn10 alloy castings have a cuboid shape with dimensions of 100×240×30. Samples for the cavitation resistance evaluation were prepared by a mechanical grinding on 100-4000 SiC papers followed by a polishing with 0.25 μm diamond slurry.

The investigated CuZn10 alloy was characterized by a solid solution single phase structure with an average grain size of ~200 μm (Fig. 1).

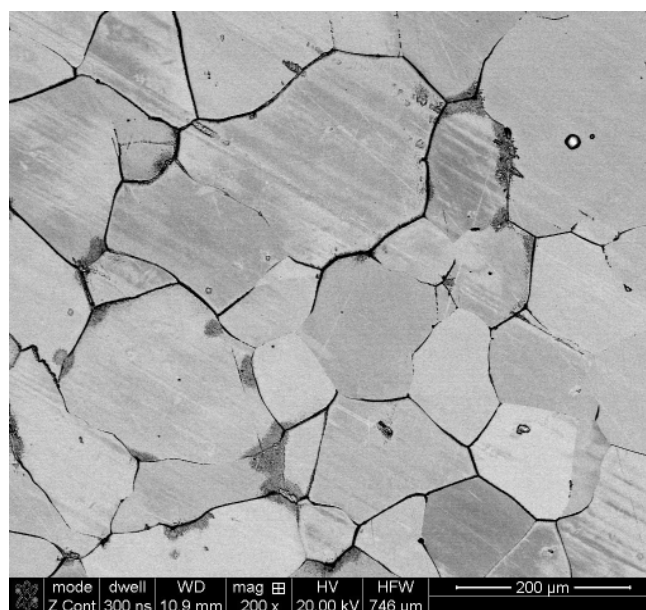


Fig. 1. A SEM microphotograph showing a microstructure of the CuZn10 alloy in as cast state

\* MARITIME UNIVERSITY OF SZCZECIN, INSTITUTE OF BASIC TECHNICAL SCIENCES, 71-650 SZCZECIN, 2-4 WILLOWA STR., POLAND

\*\* FOUNDRY RESEARCH INSTITUTE, RESEARCH CENTER OF HIGH TEMPERATUTE, 30-418 KRAKOW, 73 ZAKOPIANSKA STR., POLAND

\*\*\* MILITARY UNIVERSITY OF TECHNOLOGY, FACULTY OF ADVANCED TECHNOLOGY AND CHEMISTRY, 00-908 WARSAW, 2 KALISKIEGO STR., POLAND

# Corresponding author: r.jasionowski@am.szczecin.pl

Two types of samples were used upon the cavitation tests: one that was cut off along the transverse direction of the casting; and the second that was taken along the longitudinal direction of the casting.

Results of the EBSD examinations revealed that the former type of samples exhibit  $\langle 111 \rangle // ND$  preferred orientations (Fig. 2), while the later show  $\langle 101 \rangle // ND$  preferred orientations (Fig. 3) (ND denotes a direction normal to the exposed surface).

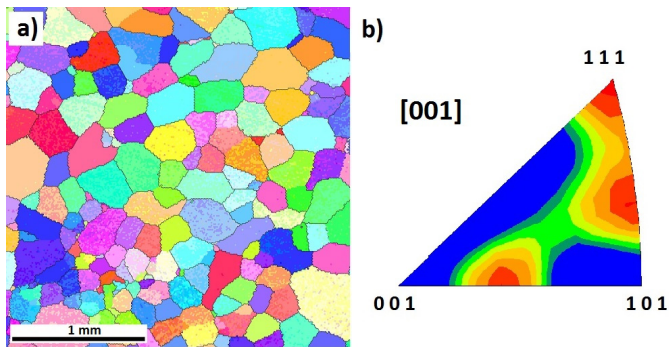


Fig. 2. Results of the electron backscatter diffraction (EBSD) analysis of the investigated CuZn10 alloy in the transverse direction: a) the inverse pole figure map, b) the inverse pole figure

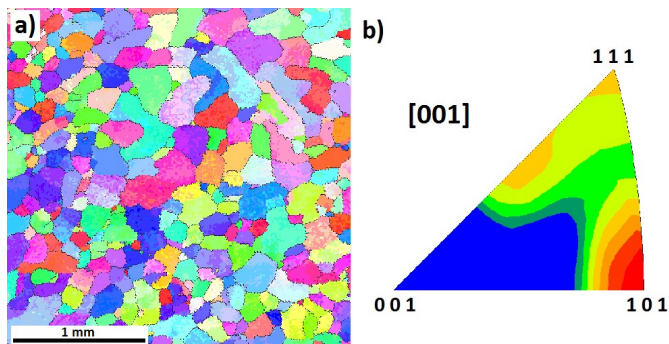


Fig. 3. Results of the electron backscatter diffraction (EBSD) analysis of the investigated CuZn10 alloy in the longitudinal direction: a) the inverse pole figure map, b) the inverse pole figure

### 3. Methodology

Cavitation erosion resistance tests were carried out on three different laboratory stands (vibration, jet-impact and flow stands). The research was conducted for three samples of as-cast CuZn10 alloy on each on laboratory stands.

#### 3.1. Vibration stand

An acoustic cavitation is a phenomenon that leads to a material destruction upon tests carried out on the vibration stand. A critical pressure is achieved by a propagation of acoustic wave that is induced by vibrations of component with attached sample (a sample may be also placed next to this component) (Fig. 4).

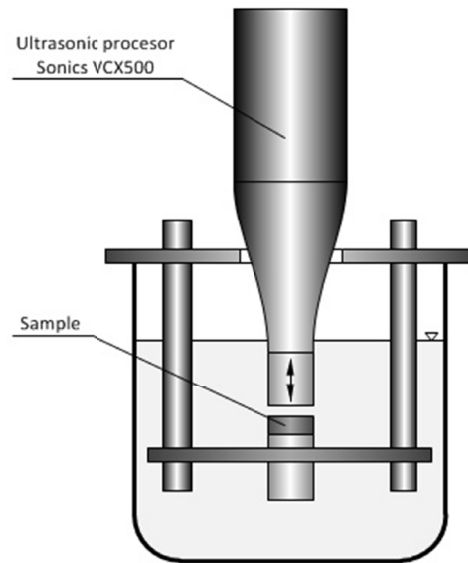


Fig. 4. The schematic drawing of the vibration stand used in the present work [7]

An electromagnetic field transducer that causes oscillating movement of the hub is a source of vibrations. The hub movement results in an erosion of sample attached to the hub or placed next to it. A course of cavitation tested on magnetron devices depends on transducer parameters, a depth of immersion, a distance between sample and transducer and physicochemical properties of liquid. The main advantages of vibration devices include a high cavitation intensity, the small size of samples and laboratory stand.

The analysis was conducted on three CuZn10 alloy samples having cylindrical shape with  $12.3 \pm 0.1$  mm diameter and  $5 \pm 0.1$  mm height. The samples were mounted in a holder placed opposite to the end of the oscillation resonator at a distance of 2.5 mm. The relative amplitude was equal to 80% of the nominal amplitude of  $124 \mu\text{m}$ . Demineralized water was used as the working liquid, maintained at a temperature of  $21\text{--}22^\circ\text{C}$ . Following exposition times were applied: 1, 5, 15, 30, 60, 90 and 120 minutes, next all samples of the CuZn10 alloy after the examination of cavitation erosion were removed from the test equipment degreased in an ultrasonic bath for a period of 3 minutes at  $30^\circ\text{C}$ , dried in the oven for 5 minutes at  $120^\circ\text{C}$  and then weighted.

#### 3.2. Jet-impact stand

A schematic drawing of typical jet-impact stand is shown in Fig. 5. This stand is composed of a rotating arm that is equipped with a sample holder. Samples rotate with a high speed and are subjected to the impact of a liquid that flows through a nozzle. The impact of flowing liquid simulates the cavitation impulses.

The intensity of destruction depends on the rotational speed of the samples, the distance between the nozzle and the samples, the flow rate and the physico-chemical properties of the liquid. Examined samples had cylindrical shape with

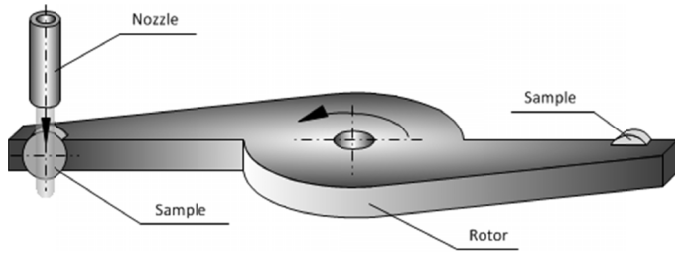


Fig. 5. The schematic drawing of the jet impact stand used in the present work [7]

$20 \pm 0.3$  mm diameter and  $6 \pm 0.5$  mm height. The samples were vertically mounted in rotor arms, parallel to the axis of water stream pumped continuously at 0.06 MPa through a 10 mm diameter nozzle located 1.6 mm away from the sample edge. The rotating samples were hitting by the water stream. Water flow of  $1.55 \text{ m}^3/\text{h}$  was constant during entire experiment. Following exposition times were applied: 15, 30, 60, 90 and 120 minutes, next all samples of the CuZn10 alloy after the examination of cavitation erosion were removed from the test equipment degreased in an ultrasonic bath for a period of 3 minutes at  $30^\circ\text{C}$ , dried in the oven for 5 minutes at  $120^\circ\text{C}$  and then weighted, than mounted again in the rotor arms, maintaining the initial position in relation to the water stream.

### 3.3. Flow stand

In flow devices the cavitation is induced by a proper design of tunnel or by a high centrifugation of a sample immersed in liquid. A shape and size of the tunnel cross sections, determining a drop of pressure and a local increase of flowing rate, should be considered as the most important features. The flowing rate in cavitation tunnels is normally within the range of 20-40 m/s, while the pressure is up to 9000 hPa. Experiments conducted on flow stands are characterized by a low cavitation intensity and a high time consumption. The schematic drawing of the flow stand used in the present paper is shown in Fig. 6.

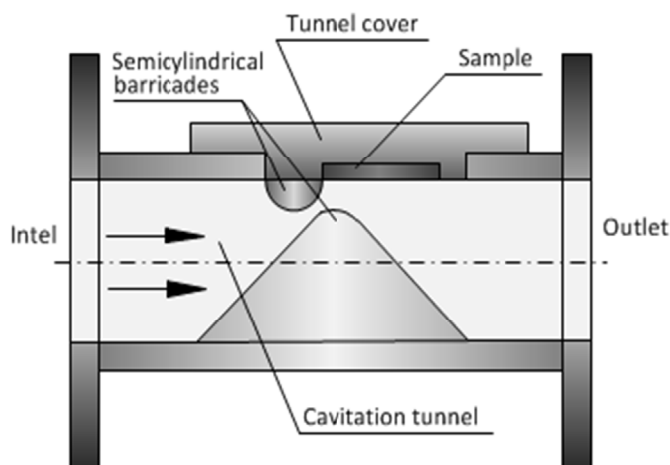


Fig. 6. The schematic drawing of the cavitation tunnel chamber of the flow stand used in the present work [7]

A cavitation tunnel chamber has dimensions of  $50 \times 50$  mm with a wedge shaped cavitation inductor. PML2 pump powered by a 15kW engine produces a working fluid pressure of approximately 5000 hPa. The working fluid was tap water with a temperature in the range of  $20\text{-}24^\circ\text{C}$ . The specimens had a parallelepiped shape with dimensions of  $30 \times 55 \times 6$  mm. Following exposition times were applied: 15, 60, 120, 180, 240, and 300 minutes. All samples of the CuZn10 alloy after the examination of cavitation erosion were removed from the test equipment degreased in an ultrasonic bath for a period of 3 minutes at  $30^\circ\text{C}$ , dried in the oven for 5 minutes at  $120^\circ\text{C}$  and then weighted.

### 3.4. Structural testing

The structural characterization of the investigated material in its initial state and after cavitation tests was carried out by using FEI Quanta 3D field emission gun scanning electron microscopy (FEG SEM EBSD system coupled with an electron backscatter diffraction (EBSD) system. For each sample the area of  $1200 \times 1200 \mu\text{m}$  was scanned with  $6 \mu\text{m}$  step size. Acquired diffraction data was then analyzed with TSL OIM Analysis 5 commercial software. The microscopic observations were conducted both on exposed surfaces, as well as on mounted metallographic cross section of samples.

## 4. Results

An analysis of cavitation tests conducted on three various laboratory stands points toward a similar course of the material destruction. A detailed study was carried out for CuZn10 samples with  $\langle 111 \rangle // \text{ND}$  or  $\langle 101 \rangle // \text{ND}$  preferred orientations upon an incubation step and upon an accelerated weight loss.

### 4.1. Vibration stand

A surface of CuZn10 samples tested on the vibration stand undergoes a strain hardening upon an initial stage of destruction process. Clearly visible effects of plastic deformation may be observed on surface of both samples ( $\langle 101 \rangle // \text{ND}$  or  $\langle 111 \rangle // \text{ND}$  (Fig. 7a)).

In a further part of the experiment, cavitation bubbles leads to a subsidence of grain interiors and an uplifting of grain boundary areas. Furthermore, first cracks and material losses are also found (Fig. 7b). Subsequently, a homogeneous erosion course is observed. However, the uplifted grain boundary regions undergoes a faster destruction than deformed grain interiors, what results in a formation of pits that have a size of  $\sim 200 \mu\text{m}$ , as well as a detachment of grain agglomerates (Fig. 7c).

The course of cavitation damage tested on vibration stand is shown as a average mass loss vs. exposure time (Fig. 8) for each samples with different preferred orientations.

Based on plotted curves, an incubation period may be dis-

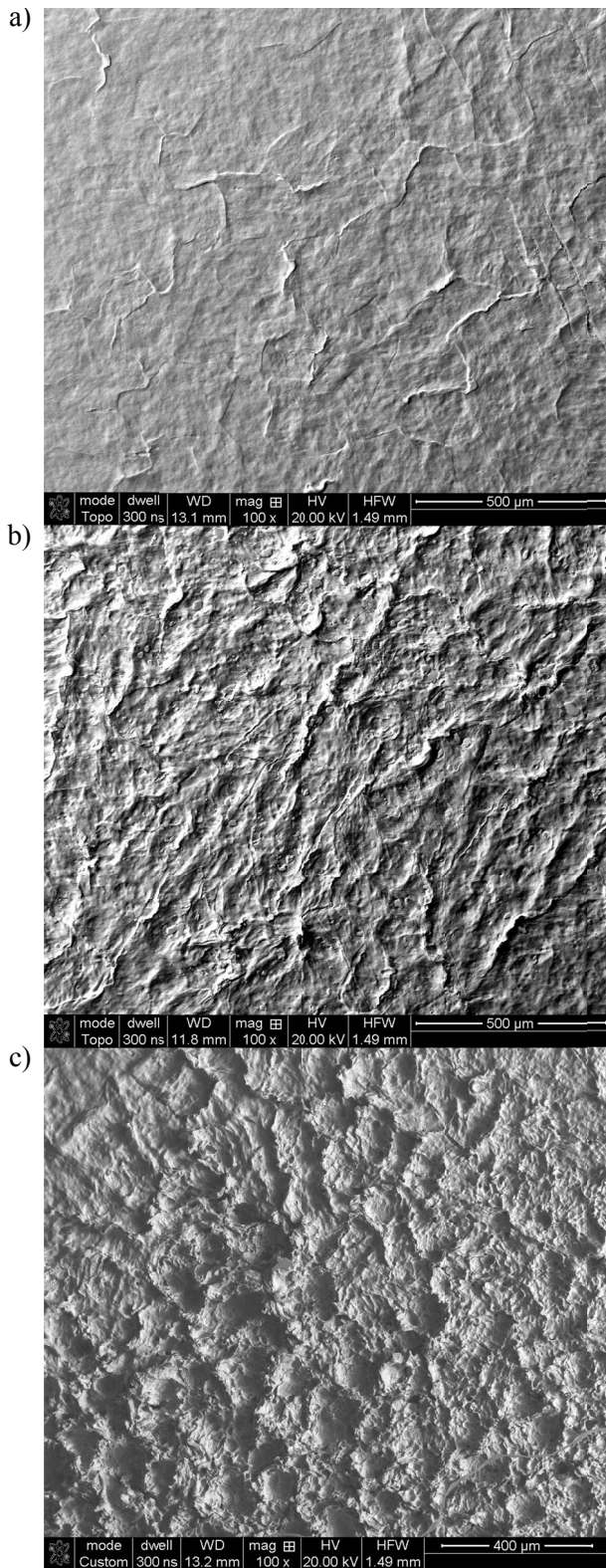


Fig. 7. The state of the CuZn10  $\langle 111 \rangle // ND$  alloy surface after test on the vibration stand: a) the effect of plastic deformation after 5 min, b) the uplifting of grain boundary zones after 15 min, c) cavities and craters on the sample surface after 90 min

tinguished, that in the present case of CuZn10 alloy is equal to 15 minutes. Despite the fact that both curves are very similar, a slightly better cavitation resistance is exhibited by samples with  $\langle 111 \rangle // ND$  preferred orientations.

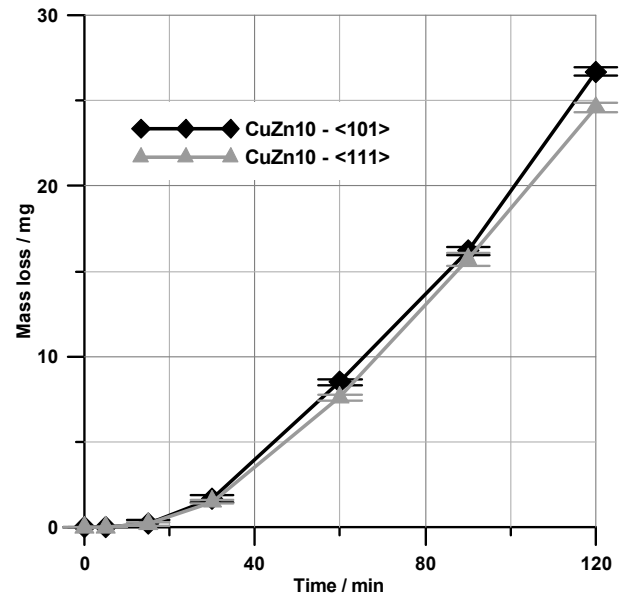


Fig. 8. Average mass loss vs. exposition time plots obtained for CuZn10 alloy tested on the vibration stand

#### 4.2. Jet-impact stand

The destruction process of CuZn10 alloy tested on the jet-impact stand follows similar course to that observed upon examinations carried out on the vibration stand. As in the previous case, the cavitation starts with a plastic deformation followed by grain boundaries uplifting (Fig. 9a). At the same time, a formation of large number of shear bands was also noted (Fig. 9b). With increasing exposure time, the uplifted grain boundaries erode uniformly, leading to a fast material loss and to the destruction of whole analyzed surface (Fig. 9c).

Three stages of destruction process upon testing on the jet-impact stand may be distinguished (namely, the incubation period, the accelerated material loss and the slower material lost) (Fig. 10).

Since the material loss starts just after few initial minutes of the test, it is hard to established the end of the incubation period. The second stage – the accelerated mass loss – is observed up to 60 minutes of the exposition, what is reflected by a change of the curves slope. The lower cavitation rate in the third period results from a partial amortization of cavitation hits by already existed pits that are filled with water.

A comparison of CuZn10 samples with different preferred orientations points toward a higher cavitation resistance of the material with the  $\langle 111 \rangle // ND$  texture, analogously as in the case of tests conducted on the vibration stand. After 120 minutes of the test, the average mass loss was 1 mg lower than that of counterparts with the  $\langle 101 \rangle // ND$  texture (Fig. 10).

#### 4.3. Flow stand

An examination of the cavitation resistance of CuZn10 alloy carried out in the cavitation tunnel (the flow stand) brought

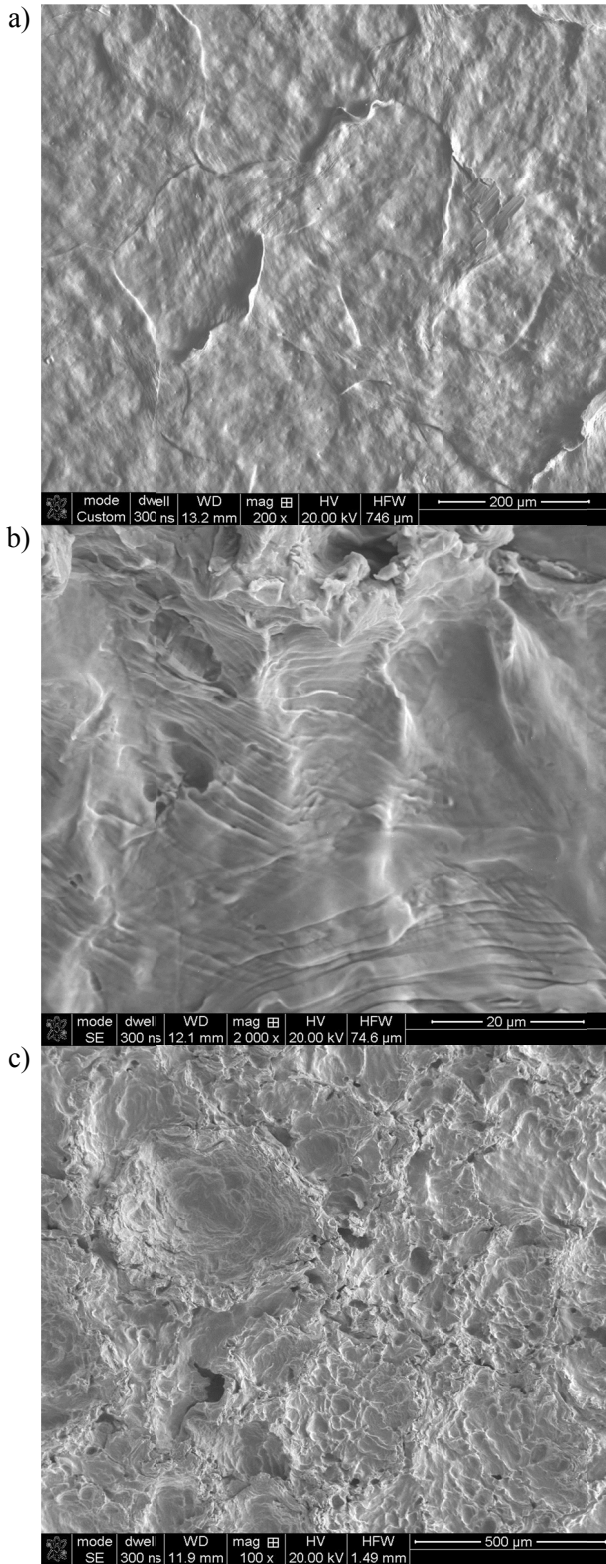


Fig. 9. The state of the CuZn10  $\langle 101 \rangle // ND$  alloy surface after test on the jet impact stand: a) the uplifting of grain boundaries zones after 5 min, b) shear bands located in near grain boundaries areas after 15 min, c) cavities and craters on the sample surface after 90 min

similar results for both types of samples. A similar course of the destruction process for  $\langle 101 \rangle // ND$  and  $\langle 111 \rangle // ND$  samples is reflected by mass loss vs. exposition time curves plotted for these samples (Fig. 11).

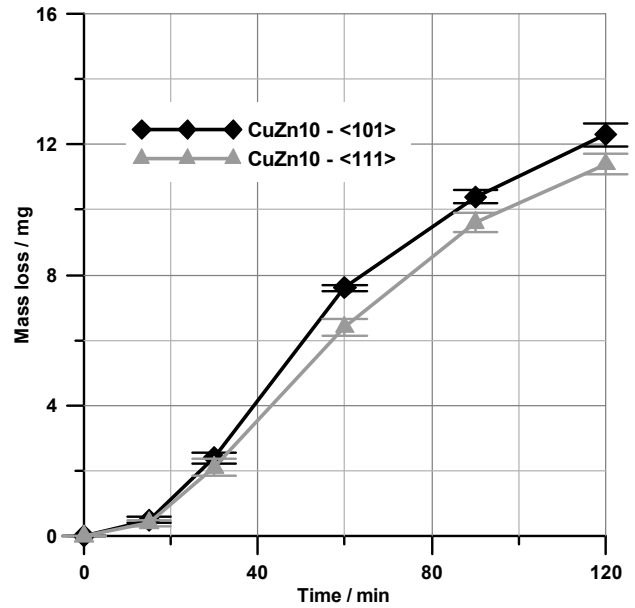


Fig. 10. Average mass loss vs. exposition time plots obtained for CuZn10 alloy tested on the jet-impact stand

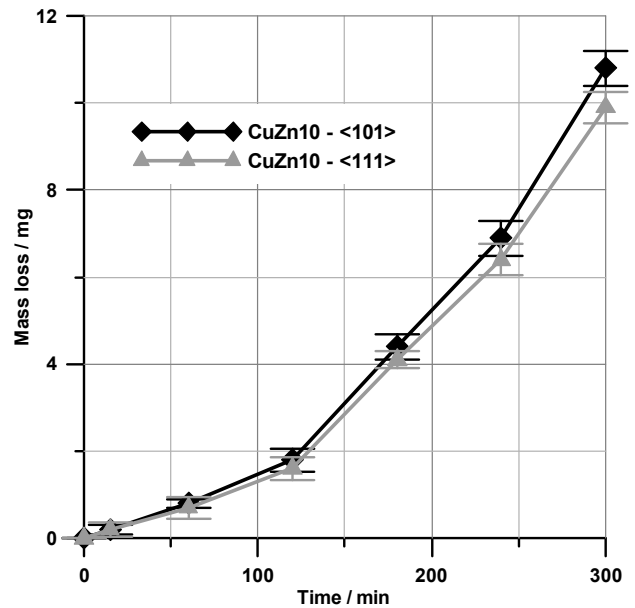


Fig. 11. Average mass loss vs. exposition time plots obtained for samples CuZn10 alloy tested on the flow stand

As in the case of previously described experiments, the destruction mechanism starts with the surface plastic deformation. Simultaneously, a large number of spherical pits was formed on the exposed sample surface (Fig. 12a).

The formation of these spherical pits is related to the presence of cavitation cloud in the tunnel and to the implosion of single bubbles near the sample surface. A further exposition leads to a more extensive plastic deformation and to a detachment of small parts of grains (Fig. 12c).

An analysis of mass change plots for both types of CuZn10 alloy samples tested on the flow stand allows distinguish two

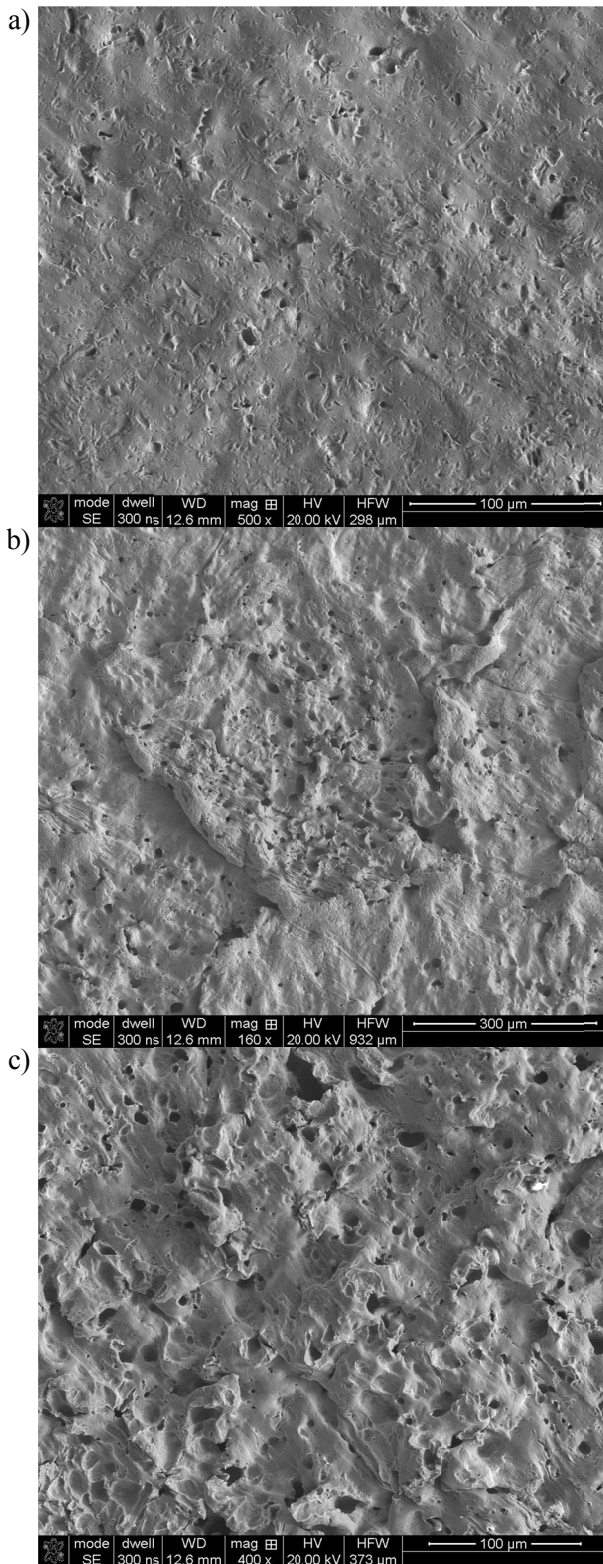


Fig. 12. The state of the CuZn10  $\langle 111 \rangle // ND$  alloy surface after test on the flow stand, a) a plastic deformation after 15 min, b) a plastic deformation and spherical pits after 120 min, c) cavities and craters on the sample surface after 240 min

stages of the material destruction (namely, the incubation period and the accelerated mass loss). A slightly higher cavitation resistance exhibited CuZn10 samples with the  $\langle 111 \rangle // ND$  crystallographic texture.

## 5. Conclusions

Results of conducted cavitation resistance evaluation of the as-cast CuZn10 alloy with  $\langle 101 \rangle // ND$  or  $\langle 111 \rangle // ND$  preferred orientations; tested on three various laboratory stands shows a similar mechanism and progress of the material destruction.

The cavitation destruction of the CuZn10 alloy takes place according to following steps:

- 1 – a surface strain hardening (reflected also by a presence of plastic deformation features such as shear bands);
- 2 – an uplifting of grain boundary areas, as an effect of the surface plastic deformation;
- 3 – a crushing of the material along uplifted grain boundaries;
- 4 – a formation of pits and craters (that size increases with the exposition time) on the material surface.

The cavitation destruction kinetics of the as-cast CuZn10 alloy, represented by mass change vs. time plots, revealed two initial stages: the incubation period and the accelerated mass loss. In the case of using the jet-impact stand, the third stage (the slower mass loss) may be also distinguished.

The cavitation resistance examinations that were carried out on three different laboratory stands (namely, vibration, jet-impact and flow stands – that are characterized by a various intensity and a way of cavitation's excitement) points toward a slightly higher cavitation resistance of the CuZn10 alloy samples with the  $\langle 111 \rangle // ND$  preferred orientations.

## Acknowledgements

Scientific work funded by the Polish Ministry of Education and Science in the years 2011-2014 as a research project No. N N507 231 040.

## REFERENCES

- [1] C.E. Brennen, *Cavitation and Bubble Dynamics*, Oxford University Press, 1995.
- [2] D.H. Trevena, *Cavitation and tension in liquids*, IOP Publishing Ltd, 1987.
- [3] M.S. Plesset, R.B. Chapman, Collapse of an Initially Spherical Vapour Cavity in the Neighbourhood of a Solid Boundary, *J. Fluid Mech.* **47** Part 2, 283-290 (1971).
- [4] E.S. Burka, Cavitation in hydraulic machinery, *Trans. Inst. Fluid-Flow Machinery* **110**, 7-19 (2002).
- [5] F.R. Young, *Cavitation*, McGraw-Hill Book Company, 1989.
- [6] O.C Jones, N. Zuber, Bubble growth in variable pressure fields, *ASME J. Heat Transfer* **100**, 453-459 (1978).
- [7] R. Jasionowski, D. Zasada, W. Polkowski, The evaluation of the cavitation damage in MgAl2Si alloy using various laboratory stands, *Solid State Phenomena* **252**, 61-70 (2016).